IEEE Access
Multidisciplinary | Rapid Review | Open Access Journal

Received September 20, 2017, accepted October 18, 2017, date of publication October 24, 2017,
date of current version November 14, 2017.

*Digital Object Identifier 10.1109/ACCESS.2017.2766079*

# Massive MIMO for Full-Duplex Cellular Two-Way Relay Network: A Spectral Efficiency Study

**ZHAOXI FANG[1], (Member, IEEE), WEI NI[2], (Senior Member, IEEE), FENG LIANG[1], PENGFEI SHAO[1], AND YAOHUI WU[1]**

[1]School of Electronics and Computer, Zhejiang Wanli University, Ningbo 315100, China
[2]Commonwealth Scientific and Industrial Research Organization, Sydney, NSW 2122, Australia

Corresponding author: Zhaoxi Fang (zhaoxifang@gmail.com)

The work was supported in part by the Natural Science Foundation of China under Grant 61401400, in part by the Natural Science Foundation of Zhejiang Province under Grant LY17F010002 and Grant LY18F010001, in part by the public welfare project of Zhejiang Province under Grant 2016C33036, and in part by the Natural Science Foundation of Ningbo City under Grant 2016A610225 and Grant 2017A610101.

**ABSTRACT** This paper presents the new analysis of the applications of massive multiple-input-multiple-output (MIMO) in full-duplex (FD) cellular two-way relay networks, and sheds valuable insights on the interactions between massive MIMO, and relay and duplex modes. Practical scenarios are considered, where massive MIMO is deployed at the base station and the relay station. Based on generic relay modes, namely, antenna-selection-based decode-and-forward (DF) relay and signal-space alignment based amplify-and-forward (AF) relay, closed-form expressions for the asymptotic signal-to-interference-plus-noise ratios (SINRs) are derived. The difference between AF and DF in the FD mode is quantified, and so is that between FD and half-duplex (HD) under the two relay modes. With massive MIMO, the superiority of DF in the FD mode is confirmed in terms of spectral efficiency. The sufficient conditions for the FD mode to outperform the HD mode are identified. The effectiveness of massive MIMO in terms of self-loop interference cancellation and inter-user interference suppression is proved. All these insightful findings are corroborated by simulations.

**INDEX TERMS** Cellular two-way relay networks, massive MIMO, full-duplex, spectral efficiency.

## I. INTRODUCTION

Being the key enabling technologies for next-generation wireless networks, full-duplex (FD) radios [1]–[8] and massive multiple-input-multiple-output (MIMO) [9], [10] have attracted extensive attention. FD radios can double the spectral efficiency of existing half-duplex (HD) radios by transmitting and receiving at the same time and frequency, attributing to recent advances in self-loop interference cancellation [11], [12]. For instance, the self-loop interference, i.e., the transmit signals of a node coupled back to the receiver of the node, has been recently suppressed by 70 to 100 dB through analog and/or digital cancellations [13]–[15]. On the other hand, massive MIMO is able to compensate for poor propagation conditions, facilitate implementing cellular networks in millimeter wave (mmWave) frequencies, and address the scarcity of communication spectrum. This is through the integration of large numbers (e.g., up to hundreds) of miniaturized antennas with significantly improved array gains [16], [17].

An important application of FD and massive MIMO is two-way relay (TWR), which has shown great potential to improve spectral efficiency at the edge of wireless systems [18]–[20]. Particularly, a cellular two-way relay network (cTWRN) is of practical interest, where a base station (BS) exchanges data with a number of remote mobile stations (MSs) outside its coverage with the assistance of a two-way relay station (RS) [21]–[24]. The BS and RS can be equipped with massive MIMO, allowing all the MSs to access the BS simultaneously and improving spectral efficiency [23], [24].

Extensive studies have been conducted on TWR in the HD mode, where a RS receives and forwards messages in two separate time slots or frequency bands [19], [20]. Recently, FD has been increasingly studied for relay, first for one-way relay (OWR) [25], [26] and then TWR [27], [28]. In the case of OWR, only the RS works in the FD mode, while the source(s) and destination(s) operate in the HD mode [25], [26]. In the case of TWR, all of the source(s), destination(s) and the relay(s) operate in the FD mode. Amplify-and-forward (AF), decode-and-forward (DF), and compress-and-forward (CF) have been considered in FD TWR networks. Unfortunately, excessive self-loop

interference and inter-stream interference (ISI) would substantially compromise the spectral efficiency [27], [28].

Lately, massive MIMO has been applied to suppress the interference in FD relay networks [26], [27], [29]–[31]. In [26], the authors maximized the energy efficiency of a multi-pair one-way FD relay network, where a FD relay was equipped with a large number of antennas to suppress the interference. In [27] and [31], the spectral and energy efficiencies of multi-pair FD TWR networks with massive MIMO were studied, showing that the use of massive MIMO at the relay can help mitigating the self-loop interference. Both the spectral and energy efficiencies increase with the number of antennas. The conditions were identified for FD TWR to outperform its HD counterpart [31]. However, these results are not applicable to cTWRNs, due to distinct network architectures. To the best of our knowledge, FD-cTWRN with massive MIMO has not yet to be studied in spite of its great potential in practice.

This paper presents analysis on the applications of massive MIMO in FD-cTWRNs, and sheds valuable insights on the interactions between massive MIMO, as well as the relay and duplex modes. Our analysis is based on generic relay modes, namely, antenna-selection based DF relay and signal-space alignment based AF relay. Closed-form expressions are derived for the asymptotic signal-to-interference-plus-noise ratios (SINRs) of the relay modes, as the numbers of antennas at the BS and RS increase. The difference between the relay modes is quantified in the FD mode, and so are those between FD and HD under each of the two relay modes. Corroborated by simulations, our analysis reveals that the SINRs increase linearly to the numbers of antennas at the BS or RS, and inversely proportionally to the number of MSs. Our analysis also shows that the use of massive MIMO allows for eliminating the self-loop interference. The sufficient conditions are identified for the DF mode (referred to as FD-DF) to outperform the AF mode (referred to as FD-AF) in terms of spectral efficiency in the FD mode. We show the superiority of FD-cTWRNs over HD-cTWRNs, and derive the conditions for FD relaying schemes to outperform their HD counterparts.

The rest of the paper is organized as follows. In Section II, the system model is presented. In Section III, FD-DF and FD-AF are described and analyzed with closed-form asymptotic spectral efficiency derived. In Section IV, the superiority of FD-cTWRNs over their HD counterparts is analytically proved. Numerical results are presented in Section V, followed by the conclusions in Section VI.

*Notation:* Boldface fonts denote vectors or matrices; the $i$-th row, the $j$-th column, and the $(i,j)$-th element of a matrix $\boldsymbol{A}$ are denoted by $\boldsymbol{a}_{(i)}$, $\boldsymbol{a}_j$, and $a(i,j)$, respectively; $\mathbb{C}^{K\times M}$ stands for the $K \times M$ complex space. $(\cdot)^*$, $(\cdot)^T$, $(\cdot)^H$ and $(\cdot)^\dagger$ denote complex conjugate, transpose, conjugate transpose and pseudo inverse, respectively; $\mathrm{tr}(\cdot)$ denotes trace; $\|\cdot\|$ denotes the Euclidean norm, and $|\cdot|$ denotes magnitude; $\mathbf{0}_{K\times M}$ is the $K \times M$ all-zero matrix; $\boldsymbol{I}_K$ denotes the $K \times K$ identity matrix; $\boldsymbol{x} \sim \mathcal{CN}(\bar{\boldsymbol{x}}, \boldsymbol{\Sigma})$ is a circularly symmetric complex Gaussian random vector $\boldsymbol{x}$ with mean $\bar{\boldsymbol{x}}$ and covariance matrix $\boldsymbol{\Sigma}$; the notation $\xrightarrow{a.s.}$ stands for "almost surely converge to"; $\mathbb{E}[\cdot]$ and $\mathbb{V}\mathrm{ar}[\cdot]$ stand for expectation and variance, respectively.

## II. SYSTEM MODEL

Fig. 1 illustrates a FD-cTWRN, where there is a BS, a RS, and $K$ MSs, all operating in the FD mode. There is no direct link between the BS and the MSs. Each MS is equipped with a single antenna. The BS is equipped with $N_B$ antennas. The relay is equipped with $N_R$ antennas. $N_R \gg K$ and $N_B \gg K$. The maximum transmit powers of the BS, RS and each MS are $P_B$, $P_R$ and $P_M$, respectively. All the BS and MSs transmit to the RS simultaneously, while the RS is transmitting previously received signals. After proper signal processing, the RS forwards the signals to the BS and MSs concurrently, while the BS and MSs are transmitting new signals to the RS.

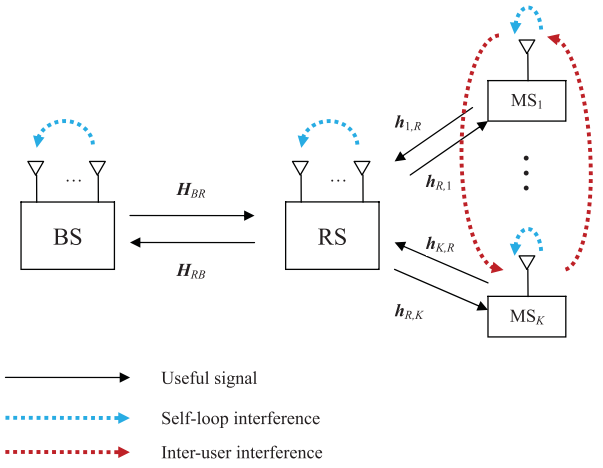


**FIGURE 1.** A full-duplex cellular two-way relay network with $K$ mobile stations.

At any time slot $n$, let $\boldsymbol{s}_B(n) = [s_{B,1}(n), \ldots, s_{B,K}(n)]^T \in \mathbb{C}^{K\times 1}$ collect the symbols of the BS to MSs with $\mathbb{E}[\boldsymbol{s}_B(n)\boldsymbol{s}_B^H(n)] = \boldsymbol{I}_K$. The transmit signals of the BS are given by

$$\boldsymbol{x}_B(n) = \boldsymbol{F}_B \boldsymbol{s}_B(n), \tag{1}$$

where $\boldsymbol{F}_B \in \mathbb{C}^{N_B\times K}$ is the beamforming matrix of the BS, satisfying the total power constraint $\mathbb{E}\left[\mathrm{tr}\left(\boldsymbol{F}_B(n)\boldsymbol{F}_B^H(n)\right)\right] = P_B$. The transmit signal of the $k$-th MS is given by

$$x_{M,k}(n) = \sqrt{P_M} s_{M,k}(n), \tag{2}$$

where $s_{M,k}(n)$ is the unit-power symbol of MS $k$.

The received signal of the RS can be written as

$$\boldsymbol{y}_R(n) = \boldsymbol{H}_{BR}\boldsymbol{x}_B(n) + \boldsymbol{H}_{MR}\boldsymbol{x}_M(n) + \boldsymbol{H}_{RR}\tilde{\boldsymbol{x}}_R(n) + \boldsymbol{z}_R(n), \tag{3}$$

where $\boldsymbol{H}_{BR} \in \mathbb{C}^{N_R\times N_B}$ and $\boldsymbol{H}_{MR} = [\boldsymbol{h}_{1,R}, \ldots, \boldsymbol{h}_{K,R}] \in \mathbb{C}^{N_R\times K}$ are the channel matrices from the BS and MSs to the RS, respectively; $\boldsymbol{H}_{RR} \in \mathbb{C}^{N_R\times N_R}$ is the self-loop interference channel at the relay. $\boldsymbol{x}_M(n) = \sqrt{P_M}\boldsymbol{s}_M(n)$ with $\boldsymbol{s}_M(n) = [s_{M,1}(n), \ldots, s_{M,k}(n)]^T$, $\tilde{\boldsymbol{x}}_R(n)$ is the self-loop interference at

the relay, and $\boldsymbol{z}_R(n) \sim \mathcal{CN}(0, \sigma^2 \boldsymbol{I}_{N_R})$ is the additive white Gaussian noise (AWGN) at the RS.

$\boldsymbol{H}_{BR} = \sqrt{\ell_B}\tilde{\boldsymbol{H}}_{BR}$ with $\ell_B$ being the path loss from the BS to the RS and $\tilde{\boldsymbol{H}}_{BR}$ collecting small-scale fading coefficients. Likewise, $\boldsymbol{H}_{MR} = \sqrt{\ell_M}\tilde{\boldsymbol{H}}_{MR}$ with $\ell_M$ being the path loss from the MSs to the RS,[1] and $\boldsymbol{H}_{RR} = \sqrt{\ell_{RL}}\tilde{\boldsymbol{H}}_{RR}$ with $\ell_{RL}$ being the path loss of the self-loop interference channel at the RS. $\tilde{\boldsymbol{H}}_{MR}$ and $\tilde{\boldsymbol{H}}_{RR}$ collect small-scale fading coefficients.

With analog and/or digital cancellation [12], [13], the self-loop interference can be substantially reduced and $\tilde{\boldsymbol{x}}_R(n)$ can be modeled as an AWGN [31], i.e., $\tilde{\boldsymbol{x}}_R(n) \sim \mathcal{CN}(0, \sigma_{RL}^2 \boldsymbol{I}_{N_R})$, where $\sigma_{RL}^2 = P_R/N_R$.

At the same time slot $n$, the transmit signal of the RS can be given by

$$\boldsymbol{x}_R(n) = f\left(\boldsymbol{y}_R(n-\tau)\right), \tag{4}$$

where $f(x)$ is a relay signal processing function to be specified later, and $\tau$ is the signal processing delay at the relay (in numbers of time slots).

We consider two relay modes, namely, DF and AF. In FD-DF, the RS decodes and then recodes the received signals. In FD-AF, the FD RS delays and forwards the received signals without decoding.

The received signals at the BS and MSs are respectively given by

$$\boldsymbol{y}_B(n) = \boldsymbol{H}_{RB}\boldsymbol{x}_R(n) + \boldsymbol{H}_{BB}\tilde{\boldsymbol{x}}_B(n) + \boldsymbol{z}_B(n); \tag{5}$$

and

$$y_{M,k}(n) = \boldsymbol{h}_{R,k}^T \boldsymbol{x}_R(n) + h_{k,k}\tilde{x}_{M,k}(n) + \sum_{i\neq k} h_{i,k}x_{M,i}(n) + z_{M,k}(n); \tag{6}$$

where $\boldsymbol{H}_{RB} \in \mathbb{C}^{N_B \times N_R}$ is the channel matrix from the RS to the BS; $\boldsymbol{h}_{R,k} \in \mathbb{C}^{N_R \times 1}$ is the channel vector from the RS to MS $k$; $\boldsymbol{H}_{BB} = \sqrt{\ell_{BL}}\tilde{\boldsymbol{H}}_{BB}$ and $h_{k,k} = \sqrt{\ell_{k,k}}\tilde{h}_{k,k}$ are the self-loop interference channels of the BS and MS $k$, respectively, and $h_{i,k} = \sqrt{\ell_{i,k}}\tilde{h}_{i,k}$ is the channel coefficient from MS $i$ to MS $k$ ($i \neq k$). $\boldsymbol{z}_B(n) \sim \mathcal{CN}(0, \sigma^2 \boldsymbol{I}_{N_B})$ and $z_{M,k}(n) \sim \mathcal{CN}(0, \sigma^2)$ are the AWGN at the BS and MS $k$, respectively. $\tilde{\boldsymbol{x}}_B(n)$ is self-loop interference at the BS and $\tilde{x}_{M,k}(n) \sim \mathcal{CN}(0, \sigma_{ML}^2)$ is the self-loop interference at MS $k$ with $\sigma_{ML}^2 = P_M$. Note that $\boldsymbol{H}_{BB}$ and $\tilde{\boldsymbol{x}}_B(n)$ depends on the specific relaying scheme, and will be given in the following.

## III. ANALYSIS OF MASSIVE MIMO ENABLED FD-cTWRNs

In this section, we individually study and compare the spectral efficiency of FD-DF and FD-AF with massive MIMO enabled at the BS and RS. Asymptotic SINRs and spectral efficiencies are inferred in closed-form with critical threshold identified for FD-DF to outperform FD-AF.

[1]For presentation clarity, we assumed that the path losses are the same for all the MSs. However, the results in this paper can be extended to FD-cTWRNs with different path losses between the MSs and the RS.

### A. FD-DF

With a large antenna array, the RS has enough degrees of freedom to suppress the inter-stream interference and to detect the messages from the BS and the MSs. For the sake of practicality, this work adopts antenna-selection at the BS, i.e., $K$ of the $N_B$ antennas at the BS are selected to send $K$ messages destined for the $K$ MSs.[2] We assume that the first $K$ antennas are selected, and the transmit beamforming matrix at the BS can therefore be given by

$$\boldsymbol{F}_B^{\mathrm{DF}} = [\sqrt{P_B/K}\boldsymbol{I}_K, \boldsymbol{0}_{K\times(N_B-K)}]^T. \tag{7}$$

As will be discussed later (in Proposition 1), the spectral efficiency of FD-DF with such simple antenna selection is independent of small-scale fading in the case that $N_B \to \infty$ and $N_R \to \infty$.

Let $\boldsymbol{H}_{BR}^{'}$ denote the first $K$ rows of $\boldsymbol{H}_{BR}$. By substituting (1) and (7) into (3), the received signal at the RS can be written as

$$\begin{aligned}\boldsymbol{y}_R(n) &= \sqrt{P_B/K}\boldsymbol{H}_{BR}^{'}\boldsymbol{s}_B(n) + \sqrt{P_M}\boldsymbol{H}_{MR}\boldsymbol{s}_M(n) \\ &\quad + \boldsymbol{H}_{RR}\tilde{\boldsymbol{x}}_R(n) + \boldsymbol{z}_R(n) \\ &= \boldsymbol{H}_{SR}\boldsymbol{s}_{BM}(n) + \boldsymbol{H}_{RR}\tilde{\boldsymbol{x}}_R(n) + \boldsymbol{z}_R(n),\end{aligned} \tag{8}$$

where $\boldsymbol{H}_{SR} = [\boldsymbol{H}_{BR}^{'}, \boldsymbol{H}_{MR}] \in \mathbb{C}^{N_R\times 2K}$, and $\boldsymbol{s}_{BM}(n) = [\sqrt{P_B/K}\boldsymbol{s}_B^T(n), \sqrt{P_M}\boldsymbol{s}_M^T(n)]^T \in \mathbb{C}^{2K\times 1}$. Here, $\boldsymbol{H}_{SR}$ can be further rewritten as

$$\boldsymbol{H}_{SR} = \tilde{\boldsymbol{H}}_{SR}\boldsymbol{\Lambda}_{SR}, \tag{9}$$

where $\tilde{\boldsymbol{H}}_{SR} \in \mathbb{C}^{N_R\times 2K}$ collects small-scale fading coefficients, and $\boldsymbol{\Lambda}_{SR} = \mathrm{diag}(\sqrt{\ell_B}\boldsymbol{I}_K, \sqrt{\ell_M}\boldsymbol{I}_K) \in \mathbb{C}^{2K\times 2K}$ collects the path losses from the BS and MSs to the RS.

Consider zero-forcing beamforming (ZFBF) at the RS to receive $\boldsymbol{y}_R(n)$. We have

$$\begin{aligned}\tilde{\boldsymbol{y}}_R(n) &= \boldsymbol{W}_{RR}^H \boldsymbol{y}_R(n) \\ &= \boldsymbol{s}_{BM}(n) + \boldsymbol{W}_{RR}^H\left(\boldsymbol{H}_{RR}\tilde{\boldsymbol{x}}_R(n) + \boldsymbol{z}_R(n)\right).\end{aligned} \tag{10}$$

where $\boldsymbol{W}_{RR}^H = \boldsymbol{H}_{SR}^{\dagger} \in \mathbb{C}^{2K\times N_R}$ is the beamforming matrix.

As the result of ZFBF, the ISI is completely removed and the RS is able to detect the messages form the BS and the MSs separately. The received SINR of $s_{B,k}(n)$ at the RS, i.e., the signals from the BS towards MS $k$, can be given by

$$\gamma_{BR,k}^{\text{FD-DF}} = \frac{P_B}{K\left(\delta_{R,k} + \mathbb{V}\mathrm{ar}\left[\boldsymbol{w}_{RR,k}^H \boldsymbol{z}_R(n)\right]\right)}, \quad k = 1, \cdots, K, \tag{11}$$

where $\boldsymbol{w}_{RR,k}$ is the $k$-th column of $\boldsymbol{W}_{RR}$, and $\delta_{R,k} = \mathbb{V}\mathrm{ar}\left[\boldsymbol{w}_{RR,k}^H \boldsymbol{H}_{RR}\tilde{\boldsymbol{x}}_R(n)\right]$ is the power of the self-loop interference after ZFBF.

[2]As will be shown in Section V, the performance gap between the proposed simple antenna-selection based FD-DF scheme and the cut-set bound is small.

Likewise, the received SINR of MS $k$'s signal at the RS can be given by

$$\gamma_{MR,k}^{\text{FD-DF}} = \frac{P_M}{\delta_{R,K+k} + \mathbb{V}\text{ar}\left[\boldsymbol{w}_{RR,K+k}^H \boldsymbol{z}_R(n)\right]}, \quad k = 1, \cdots, K, \quad (12)$$

where $\delta_{R,K+k} = \mathbb{V}\text{ar}\left[\boldsymbol{w}_{RR,K+k}^H \boldsymbol{H}_{RR}\tilde{\boldsymbol{x}}_R(n)\right]$ is the power of the self-loop interference after ZFBF.

With a large number of antennas at the RS, we have

$$\begin{aligned}\delta_{R,k} &= \sigma_{RL}^2 \mathbb{E}\left[\boldsymbol{w}_{RR,k}^H \boldsymbol{H}_{RR}\boldsymbol{H}_{RR}^H \boldsymbol{w}_{RR,k}\right] \\ &= \ell_{RL} N_R \sigma_{RL}^2 \mathbb{E}\left[\|\boldsymbol{w}_{RR,k}\|^2\right] \\ &= \frac{\ell_{RL} P_R}{(N_R - K)\ell_B}, \end{aligned} \quad (13)$$

which is due to the fact that $\frac{1}{N_R}\boldsymbol{H}_{RR}\boldsymbol{H}_{RR}^H \simeq \ell_{RL}\boldsymbol{I}_{N_R}$ for $N_R \to \infty$. Likewise, for $N_R \to \infty$, we have

$$\delta_{R,K+k} = \frac{\ell_{RL} P_R}{(N_R - K)\ell_M}. \quad (14)$$

Note that (13) and (14) reveal that $\delta_{R,k} \to 0$ and $\delta_{R,K+k} \to 0$, as $N_R \to +\infty$; i.e., the self-loop interference can be cancelled when the RS is equipped with a large number of antennas.

Now, based on (10), the RS can estimate the symbols from the BS and MSs as $\hat{s}_{B,k}(n)$ and $\hat{s}_{M,k}(n)$, respectively, $k = 1, \ldots, K$. Then, it recodes the signals into $\boldsymbol{s}_R(n) = [s_{R,1}(n), \ldots, s_{R,K}(n)]^T$, and forwards them using ZFBF to suppress ISI among the MSs, where $s_{R,k}(n) = \hat{s}_{B,k}(n) \oplus \hat{s}_{M,k}(n)$, $k = 1, \ldots, K$. The transmit signal of the RS is given by

$$\boldsymbol{x}_R(n) = \alpha_R^{\text{DF}} \boldsymbol{H}_{RM}^{\dagger} \boldsymbol{s}_R(n - \tau), \quad (15)$$

where $\alpha_R^{\text{DF}}$ is an adjustable coefficient for meeting the transmit power constraint of the RS, and can be given by

$$\alpha_R^{\text{DF}} = \sqrt{\frac{P_R}{\mathbb{E}\left[\text{tr}\left(\boldsymbol{H}_{RM}^{\dagger}\boldsymbol{H}_{RM}^{\dagger H}\right)\right]}}. \quad (16)$$

The received signals at the BS and MS $k$ are respectively given by

$$\boldsymbol{y}_B(n) = \alpha_R^{\text{DF}} \boldsymbol{H}_{RB}\boldsymbol{H}_{RM}^{\dagger}\boldsymbol{s}_R(n - \tau) + \boldsymbol{H}_{BB}\tilde{\boldsymbol{x}}_B(n) + \boldsymbol{z}_B(n); \quad (17)$$

and

$$\begin{aligned}\boldsymbol{y}_{M,k}(n) = \alpha_R^{\text{DF}} \boldsymbol{s}_R(n - \tau) + h_{k,k}\tilde{x}_{M,k}(n) \\ + \sum_{i \neq k} h_{i,k} x_{M,i}(n) + z_{M,k}(n). \end{aligned} \quad (18)$$

The second term on the right-hand side (RHS) of (17) is the self-loop interference at the BS, where $\boldsymbol{H}_{BB} \in \mathbb{C}^{N_B \times K}$ and $\tilde{\boldsymbol{x}}_B(n) \sim \mathcal{CN}(0, \sigma_{BL}^2 \boldsymbol{I}_K)$ denotes the self-loop channel and the self-loop interference with $\sigma_{BL}^2 = P_B/K$, respectively. The second and third terms on the RHS of (18) are the self-loop interference and ISI at MS $k$, respectively.

Consider ZFBF for the reception at the BS. The beamforming matrix is $\boldsymbol{W}_B^H = \left(\boldsymbol{H}_{RB}\boldsymbol{H}_{RM}^{\dagger}\right)^{\dagger}$. From (17), the receive SINR of MS $k$'s signal at the BS can be given by

$$\gamma_{RB,k}^{\text{FD-DF}} = \frac{(\alpha_R^{\text{DF}})^2}{\delta_{B,k} + \mathbb{V}\text{ar}\left[\boldsymbol{w}_{B,k}^H \boldsymbol{z}_B(n)\right]}, \quad (19)$$

where $\boldsymbol{w}_{B,k}$ is the $k$-th column of $\boldsymbol{W}_B$, and $\delta_{B,k} = \mathbb{V}\text{ar}\left[\boldsymbol{w}_{B,k}^H \boldsymbol{H}_{BB}\tilde{\boldsymbol{x}}_B(n)\right]$ is the power of the self-loop interference after ZFBF. With a large number of receive antennas at the BS, i.e., $N_B \to \infty$, $\delta_{B,k}$ can be written as

$$\begin{aligned}\delta_{B,k} &= \sigma_{BL}^2 \mathbb{E}\left[\boldsymbol{w}_{B,k}^H \boldsymbol{H}_{BB}\boldsymbol{H}_{BB}^H \boldsymbol{w}_{B,k}\right] \\ &= \frac{\ell_M \ell_{BL} N_R P_B}{\ell_B N_B}. \end{aligned} \quad (20)$$

From (20), we have

$$\frac{\delta_{B,k}}{(\alpha_R^{\text{DF}})^2} = \frac{K\ell_{BL}P_B}{\ell_B N_B} \to 0, \quad \text{as } N_B \to +\infty. \quad (21)$$

In other words, the self-loop interference at the BS becomes negligible, and a large number of antennas in massive MIMO is able to eliminate the self-loop interference at the BS.

From (18), the receive SINR at MS $k$ can be given by

$$\gamma_{RM,k}^{\text{FD-DF}} = \frac{(\alpha_R^{\text{DF}})^2}{|h_{k,k}|^2\sigma_{ML}^2 + P_M \sum_{i \neq k} |h_{i,k}|^2 + \sigma^2}. \quad (22)$$

where the ISI and self-loop interference cannot be mitigated, since each MS has only a single antenna.

By combining (11), (12), (19) and (22), the achievable spectral efficiency of FD-DF can be given by

$$\begin{aligned}R_{\text{sum}}^{\text{FD-DF}} = \sum_{k=1}^{K} [\mathcal{C}(\min(\gamma_{BR,k}^{\text{FD-DF}}, \gamma_{RM,k}^{\text{FD-DF}})) \\ + \mathcal{C}(\min(\gamma_{MR,k}^{\text{FD-DF}}, \gamma_{RB,k}^{\text{FD-DF}}))], \end{aligned} \quad (23)$$

where $\mathcal{C}(x) = \log_2(1 + x)$.

*Proposition 1:* In the case that $N_B \to +\infty$ and $N_R \to +\infty$, the receive SINRs of FD-DF almost surely converge to

$$\frac{\gamma_{BR,k}^{\text{FD-DF}}}{N_R} \xrightarrow{a.s.} \frac{\ell_B P_B}{K\sigma_R^2}; \quad (24a)$$

$$\frac{\gamma_{MR,k}^{\text{FD-DF}}}{N_R} \xrightarrow{a.s.} \frac{\ell_M P_M}{\sigma_R^2}; \quad (24b)$$

$$\frac{\gamma_{RB,k}^{\text{FD-DF}}}{N_B} \xrightarrow{a.s.} \frac{\ell_B P_R}{K\sigma_B^2}; \quad (24c)$$

$$\frac{\gamma_{RM,k}^{\text{FD-DF}}}{N_R} \xrightarrow{a.s.} \frac{\ell_M P_R}{K\sigma_k^2}; \quad (24d)$$

where $k = 1, \ldots, K$, $\sigma_B^2 = \sigma^2 + \ell_{BL}P_B$; $\sigma_R^2 = \sigma^2 + \ell_{RL}P_R$; and $\sigma_k^2 = \sigma^2 + P_M \sum_{i=1}^{K} \ell_{i,k}$, $\forall k$.

*Proof:* This proposition can be proved using the law of large numbers and the assumption of independent fading channels. For details, see Appendix A. ∎

Proposition 1 reveals that the small-scale fading does not affect the spectral efficiency of FD-DF if both the BS and RS are equipped with massive MIMO. Despite the existence of self-loop interference and ISI, the receive SINRs at the RS and MSs increase with $N_R$, and the receive SINRs at the BS increases with $N_B$. To this end, the spectral efficiency of FD-DF improves with the numbers of antennas at the BS and RS in cTWRNs. This confirms the effectiveness of the simple antenna selection described at the beginning of this section.

### B. FD-AF

To allow the RS to forward signals without decoding, signal space alignment based linear precoding [24] is considered at the BS to align the received signals from the BS and MSs at the RS. The beamforming matrix at the BS can be given by

$$\boldsymbol{F}_B^{\mathrm{AF}} = \alpha_B \left(\boldsymbol{H}_{MR}^{\dagger}\boldsymbol{H}_{BR}\right)^{\dagger}, \tag{25}$$

where $\alpha_B$ is an adjustable coefficient to guarantee the power constraint at the BS, i.e., $\mathbb{E}\left[\mathrm{tr}\left(\boldsymbol{F}_B^{\mathrm{AF}}\left(\boldsymbol{F}_B^{\mathrm{A}}\right)^H\right)\right] = P_B$.

Without decoding, the RS retransmits the received signal:

$$\boldsymbol{x}_R(n) = \alpha_R^{\mathrm{AF}}\boldsymbol{H}_{RM}^{\dagger}\boldsymbol{H}_{MR}^{\dagger}\boldsymbol{y}_R(n-\tau), \tag{26}$$

where $\alpha_R^{\mathrm{AF}}$ is an adjustable coefficient to guarantee the power constraint at the RS.

From (5), (25) and (26), the received signals at the BS and MSs can be given respectively by

$$\begin{aligned}\boldsymbol{y}_B(n) &= \alpha_R^{\mathrm{AF}}\boldsymbol{H}_{RB}\boldsymbol{H}_{RM}^{\dagger}\left[\alpha_B\boldsymbol{s}_B(n-\tau)+\sqrt{P_M}\boldsymbol{s}_M(n-\tau)\right]\\ &\quad+\alpha_R^{\mathrm{AF}}\boldsymbol{H}_{RB}\boldsymbol{H}_{RM}^{\dagger}\left[\boldsymbol{H}_{MR}^{\dagger}\left(\boldsymbol{H}_{RR}\tilde{\boldsymbol{x}}_R(n-\tau)+\boldsymbol{z}_R(n-\tau)\right)\right]\\ &\quad+\boldsymbol{H}_{BB}\tilde{\boldsymbol{x}}_B(n)+\boldsymbol{z}_B(n);\end{aligned} \tag{27}$$

and

$$\begin{aligned}\boldsymbol{y}_{M,k}(n) &= \alpha_R^{\mathrm{AF}}\left[\alpha_B\boldsymbol{s}_B(n-\tau)+\sqrt{P_M}\boldsymbol{s}_M(n-\tau)\right]\\ &\quad+\alpha_R^{\mathrm{AF}}\left[\boldsymbol{v}_{RR,k}^H\left(\boldsymbol{H}_{RR}\tilde{\boldsymbol{x}}_R(n-\tau)+\boldsymbol{z}_R(n-\tau)\right)\right]\\ &\quad+h_{k,k}\tilde{x}_{M,k}(n)+\sum_{i\neq k}h_{i,k}x_{M,i}(n)+z_{M,k}(n);\end{aligned} \tag{28}$$

where $\boldsymbol{v}_{RR,k}$ is the $k$-th column of $\left(\boldsymbol{H}_{MR}^{\dagger}\right)^H$, $\boldsymbol{H}_{BB}\in\mathbb{C}^{N_B\times N_B}$ denotes the self-loop channel, and $\tilde{\boldsymbol{x}}_B(n)\sim\mathcal{CN}(0,\sigma_{BL}^2\boldsymbol{I}_{N_B})$ denotes self-loop interference with $\sigma_{BL}^2 = P_B/N_B$, respectively. The term involving $\boldsymbol{s}_B(n-\tau)$ in (27) is the self-interference at the BS, which is known to the BS and can be self-canceled prior to signal detection at the BS. After canceling the self-interference, the BS can employ ZFBF, i.e., $\boldsymbol{W}_B^H = \left(\boldsymbol{H}_{RB}\boldsymbol{H}_{RM}^{\dagger}\right)^{\dagger}$, to detect the signals from the MSs.

From (27), the receive SINR of MS $k$'s signal at the BS can be given by

$$\gamma_{B,k}^{\text{FD-AF}} = \frac{(\alpha_R^{\mathrm{AF}})^2 P_M}{(\alpha_R^{\mathrm{AF}})^2(\mu_{R,k}+\rho_{R,k})+\delta_{B,k}+\mathbb{V}\mathrm{ar}\left[\boldsymbol{w}_{B,k}^H\boldsymbol{z}_B(n)\right]}, \tag{29}$$

where $\mu_{R,k} = \mathbb{V}\mathrm{ar}\left[\boldsymbol{v}_{RR,k}^H\boldsymbol{H}_{RR}\tilde{\boldsymbol{x}}_R(n-\tau)\right]$ is the power of the self-loop interference propagated from the RS, and $\rho_{R,k} = \mathbb{V}\mathrm{ar}\left[\boldsymbol{v}_{RR,k}^H\boldsymbol{z}_R(n-\tau)\right]$ is the power of the noise propagated from the RS.

From (28), after canceling the self-interference at MS $k$ , the receive SINR is given by

$$\gamma_{M,k}^{\text{FD-AF}} = \frac{(\alpha_R^{\mathrm{AF}})^2\alpha_B^2}{(\alpha_R^{\mathrm{AF}})^2(\mu_{R,k}+\rho_{R,k})+P_M\sum_{i=1}^{K}|h_{i,k}|^2+\sigma^2}. \tag{30}$$

By combining (29) and (30), the achievable spectral efficiency of FD-AF can finally be given by

$$R_{\mathrm{sum}}^{\text{FD-AF}} = \sum_{k=1}^{K}[\mathcal{C}(\gamma_{B,k}^{\text{FD-AF}})+\mathcal{C}(\gamma_{M,k}^{\text{FD-AF}})]. \tag{31}$$

*Proposition 2:* In the case of $N_R\to\infty$ and $N_B\to\infty$, the receive SINRs at the BS and MSs of FD-AF almost surely converge to

$$\frac{\gamma_{B,k}^{\text{FD-AF}}}{N_R}\xrightarrow{a.s.}\frac{\alpha\ell_M\ell_B P_R P_M}{\alpha\ell_B P_R\sigma_R^2+(\alpha\ell_B P_B+\ell_M K P_M)\sigma_B^2}; \tag{32a}$$

$$\frac{\gamma_{M,k}^{\text{FD-AF}}}{N_R}\xrightarrow{a.s.}\frac{\alpha\ell_M\ell_B P_B P_R}{K\left[\ell_M P_R\sigma_R^2+(\alpha\ell_B P_B+\ell_M K P_M)\sigma_k^2\right]}; \tag{32b}$$

where $k=1,\ldots,K$, and $\alpha$ specifies the BS-to-RS antenna ratio, i.e., $\alpha = N_B/N_R$.

*Proof:* See Appendix B. ∎

From Proposition 2, we see that small-scale fading can be suppressed in the presence of massive MIMO, and the receive SINR increases with the numbers of antennas as it does in FD-DF (as revealed in Proposition 1).

### C. COMPARISON BETWEEN FD-DF AND FD-AF

In the following, a comparison study is carried out between FD-DF and FD-AF, and critical conditions are identified for FD-DF to outperform FD-AF in terms of spectral efficiency.

*Proposition 3:* In the case that $N_B\to\infty$ and $N_R\to\infty$, FD-DF is able to achieve higher spectral efficiency than FD-AF if the following condition holds:

$$P_B \geq \frac{\ell_M\sigma^2}{\ell_B\sigma_{\min}^2}P_R, \tag{33}$$

where $\sigma_{\min}^2 = \min_{k=1,\cdots,K}\{\sigma_k^2\}$.

*Proof:* We can start with the downlink transmission, i.e., from the BS to the MSs. If (33) holds, $P_B \geq \frac{\ell_M\sigma^2}{\ell_B\sigma_k^2}P_R$, $\forall k$. Then, we have $\gamma_{BR,k}^{\text{FD-DF}} \geq \gamma_{RM,k}^{\text{FD-DF}}$, $\forall k$, i.e., the bottleneck of the transmission of FD-DF is the hop from the RS to the MSs.

Therefore, in the downlink, the achievable spectral efficiency is given by

$$R_{\text{sum,DL}}^{\text{FD-DF}} = \sum_{k=1}^{K} \mathcal{C}(\min(\gamma_{BR,k}^{\text{FD-DF}}, \gamma_{RM,k}^{\text{FD-DF}})) = \sum_{k=1}^{K} \mathcal{C}(\gamma_{RM,k}^{\text{FD-DF}}). \quad (34)$$

For FD-AF, it is easy to show that the downlink SINRs $\gamma_{M,k}^{\text{FD-AF}} < \gamma_{RM,k}^{\text{FD-DF}}, \forall k$. Hence, FD-DF achieves a higher spectral efficiency than FD-AF in the downlink of cTWRNs.

Proceed with the uplink. We can show that $\gamma_{B,k}^{\text{FD-AF}} < \gamma_{MR,k}^{\text{FD-DF}}, \forall k$, and $\gamma_{B,k}^{\text{FD-AF}} < \gamma_{RB,k}^{\text{FD-DF}}, \forall k$, always hold. As a result, we can conclude that FD-DF bypasses FD-AF as long as (33) withstands. ■

It is worth mentioning that in practical cellular networks, the transmit power of the BS is typically much higher than that of the RS. Moreover, the RS is generally placed with a line-of-sight (LoS) towards the BS. For these reasons, (33) can be typically satisfied, and FD-DF can outperform FD-AF in most practical cases. On the other hand, FD-DF has a higher complexity and cost than FD-AF, since no decoding or recoding operation is involved in FD-AF.

### D. POWER SCALING CASE

We proceed to show the power savings at the MSs offered by massive MIMO in FD-cTWRNs. Particularly, the transmit power of the MSs can decrease inversely proportionally with the spectral efficiency unaffected, as the number of antennas increases at the RS.

*Proposition 4:* Consider a power scaling case that $P_B$ and $P_R$ are fixed, while the transmit power of each MS $P_M$ scales with the number of RS antennas as $P_M = P_M^0/N_R$, where $P_M^0$ is a constant. In the case that $N_B \to +\infty$ and $N_R \to +\infty$, the receive SINRs of FD-DF almost surely converge to

$$\frac{\gamma_{BR,k}^{\text{FD-DF}}}{N_R} \xrightarrow{a.s.} \frac{\ell_B P_B}{K\sigma_R^2}; \quad (35a)$$

$$\gamma_{MR,k}^{\text{FD-DF}} \xrightarrow{a.s.} \frac{\ell_M P_M^0}{\sigma_R^2}; \quad (35b)$$

$$\frac{\gamma_{RB,k}^{\text{FD-DF}}}{N_B} \xrightarrow{a.s.} \frac{\ell_B P_R}{K\sigma_B^2}; \quad (35c)$$

$$\frac{\gamma_{RM,k}^{\text{FD-DF}}}{N_R} \xrightarrow{a.s.} \frac{\ell_M P_R}{K\sigma^2}. \quad (35d)$$

The receive SINRs of FD-AF at the BS and MSs almost surely converge to

$$\gamma_{B,k}^{\text{FD-AF}} \xrightarrow{a.s.} \frac{\ell_M P_R P_M^0}{P_R\sigma_R^2 + P_B\sigma_B^2}; \quad (36a)$$

$$\frac{\gamma_{M,k}^{\text{FD-AF}}}{N_R} \xrightarrow{a.s.} \frac{\alpha\ell_M\ell_B P_B P_R}{K\left[\ell_M P_R\sigma_R^2 + \alpha\ell_B P_B\sigma^2\right]}. \quad (36b)$$

From (35b) and (36a), we see that the receive SINRs $\gamma_{MR,k}^{\text{FD-DF}}$ and $\gamma_{B,k}^{\text{FD-AF}}$, $k = 1, \ldots, K$, only depend on $P_M^0$, not on $N_R$. In other words, the reduction of $P_M$ can be compensated for by increasing $N_R$ inversely proportionally, while the receive SINRs at the RS, or the spectral efficiency, remain unaffected in the uplink for both FD-DF and FD-AF. This suggests that with the numbers of antennas at the BS and RS approaching infinite, the transmit power of the MSs can be made arbitrary small, while preserving the spectral efficiency in the uplink.

## IV. COMPARISON BETWEEN HD AND FD cTWRNs

In this section, comparison studies are carried out between FD-cTWRNs and their HD counterparts which necessitate two successive time slots to accomplish a cycle of TWR [21], [22]. The superiority of the FD mode to the HD mode is proved in terms of spectral efficiency.

### A. FD-DF VERSUS HD-DF

Consider HD-DF in cTWRNs. The achievable spectral efficiency is given by [23]

$$R_{\text{sum}}^{\text{HD-DF}} = \frac{K}{2}\log_2\left[1 + \frac{\min\left(\ell_B N_R P_B, \ell_M N_R P_R\right)}{K\sigma^2}\right] + \frac{K}{2}\log_2\left[1 + \frac{\min\left(KN_R\ell_M P_M, \ell_B N_B P_R\right)}{K\sigma^2}\right], \quad (37)$$

where the coefficient $1/2$ is due to the use of the HD mode.

From (23), (24) and (37), we conclude that:

*Proposition 5:* FD-DF can always outperform HD-DF in cTWRNs in the case that $N_B \to \infty$ and $N_R \to \infty$.

*Proof:* Let $\sigma_{k,\max}^2 = \max\{\sigma_R^2, \sigma_k^2\}$ and $\sigma_{\text{DL,max}}^2 = \max_{k=1,\cdots,K}\{\sigma_{k,\max}^2\}$. In the downlink, the achievable spectral efficiency of FD-DF is lower bounded by

$$R_{\text{sum,DL}}^{\text{FD-DF}} = \sum_{k=1}^{K} \mathcal{C}(\min(\gamma_{BR,k}, \gamma_{RM,k})) \geq K\log_2\left[\frac{\min\left(\ell_B N_R P_B, \ell_M N_R P_R\right)}{K\sigma_{\text{DL,max}}^2}\right]. \quad (38)$$

Likewise, let $\sigma_{\text{UL,max}}^2 = \max\{\sigma_R^2, \sigma_B^2\}$. In the uplink, the achievable spectral efficiency of FD-DF is lower bounded by

$$R_{\text{sum,UL}}^{\text{FD-DF}} = \sum_{k=1}^{K} \mathcal{C}(\min(\gamma_{MR,k}, \gamma_{RB,k})) \geq K\log_2\left[\frac{\min\left(KN_R\ell_M P_M, \ell_B N_B P_R\right)}{K\sigma_{\text{UL,max}}^2}\right]. \quad (39)$$

From (37), (38) and (39), we see that the gain of FD-DF over HD-DF in spectral efficiency is lower bounded by

$$\begin{aligned}\Delta R_{\text{sum}}^{\text{DF}} &= R_{\text{sum}}^{\text{FD-DF}} - R_{\text{sum}}^{\text{HD-DF}} \\ &\geq R_{\text{sum,DL}}^{\text{FD-DF,LB}} + R_{\text{sum,UL}}^{\text{FD-DF,LB}} - R_{\text{sum}}^{\text{HD-DF}} \\ &= \frac{K}{2}\log_2\left[\frac{\sigma^2\min\left(\ell_B N_R P_B, \ell_M N_R P_R\right)}{K\sigma_{\text{DL,max}}^4}\right] \\ &\quad + \frac{K}{2}\log_2\left[\frac{\sigma^2\min\left(KN_R\ell_M P_M, \ell_B N_B P_R\right)}{K\sigma_{\text{UL,max}}^4}\right]. \quad (40)\end{aligned}$$

which is positive, i.e., $\Delta R_{\text{sum}}^{\text{DF}} > 0$, if $N_B \to +\infty$ and $N_R \to +\infty$. Here, $R_{sum,\,DL}^{FD-DF,\,LB}$ and $R_{sum,\,UL}^{FD-DF,\,LB}$ are the RHSs of the inequalities in (38) and (39), respectively. ■

The above result shows that FD-DF can always achieve a higher spectral efficiency than HD-DF even if the self-loop interference cannot be perfectly canceled, in the presence of massive MIMO at the BS and RS.

From (23), (24) and (37), we can also show that:

*Proposition 6:* FD-DF achieves a higher spectral efficiency than HD-DF when the number of antennas at the BS and the RS satisfies:

$$N_R \geq \max\left\{\frac{K\sigma_R^4}{\ell_B P_B \sigma^2}, \frac{\sigma_R^4}{\ell_M P_M \sigma^2}, \max_k \frac{K\sigma_k^4}{\ell_M P_R \sigma^2}\right\},$$
$$N_B \geq \frac{K\sigma_B^4}{\ell_B P_R \sigma^2}. \tag{41}$$

### B. FD-AF VERSUS HD-AF

In the case that $N_B \to \infty$ and $N_R \to \infty$, the achievable spectral efficiency of HD-AF is given by [24]

$$R_{\text{sum}}^{\text{HD-AF}} = \frac{1}{2}\sum_{k=1}^{K}[\mathcal{C}(\gamma_{B,k}^{\text{HD-AF}}) + \mathcal{C}(\gamma_{M,k}^{\text{HD-AF}})], \tag{42}$$

where the coefficient $1/2$ is due to the use of the HD mode, and the receive SINRs are given by

$$\frac{\gamma_{B,k}^{\text{HD-AF}}}{N_R} \xrightarrow{a.s.} \frac{\alpha\ell_M\ell_B P_R P_M}{(\alpha\ell_B(P_R+P_B)+\ell_M K P_M)\sigma^2},$$
$$\frac{\gamma_{M,k}^{\text{HD-AF}}}{N_R} \xrightarrow{a.s.} \frac{\alpha\ell_M\ell_B P_B P_R}{K(\ell_M P_R+\alpha\ell_B P_B+\ell_M K P_M)\sigma^2}, \tag{43}$$

$k = 1, \ldots, K$.

From (31), (32), (42) and (43), the gain of FD-AF over HD-AF is lower bounded by

$$\begin{aligned}\Delta R_{\text{sum}}^{\text{AF}} &= R_{\text{sum}}^{\text{FD-AF}} - R_{\text{sum}}^{\text{HD-AF}} \\ &\geq \frac{K}{2}\log_2\left[\frac{\alpha\sigma^2 N_R\ell_M\ell_B P_B P_R}{K\left(\ell_M P_R+\alpha\ell_B P_B+\ell_M K P_M\right)\sigma_{\text{DL,max}}^4}\right] \\ &\quad + \frac{K}{2}\log_2\left[\frac{\alpha\sigma^2 N_R\ell_M\ell_B P_R P_M}{(\alpha\ell_B P_R+\alpha\ell_B P_B+\ell_M K P_M)\sigma_{\text{UL,max}}^4}\right].\end{aligned} \tag{44}$$

where we can show that $\Delta R_{\text{sum}}^{\text{AF}} > 0$ if $N_B \to +\infty$ and $N_R \to +\infty$. As a result, we can conclude that:

*Proposition 7:* FD-AF can always outperform HD-AF in cTWRNs in the case that $N_B \to \infty$ and $N_R \to \infty$.

From (32) and (43), we can also show that:

*Proposition 8:* FD-AF achieves a higher spectral efficiency than HD-AF when the number of antennas at the BS and the RS satisfies:

$$N_R \geq \frac{\left(P_R\sigma_R^2 + P_B\sigma_B^2\right)^2}{\ell_M P_R P_M (P_B+P_R)\sigma^2},$$
$$N_B \geq \frac{K N_R\ell_M P_R\sigma_{\text{DL,max}}^4}{\ell_B P_B\left(N_R\ell_M P_R\sigma^2 - K\sigma_{\text{DL,max}}^4\right)}. \tag{45}$$

## V. NUMERICAL RESULTS

In the simulations, the path losses are modeled as $\ell_B = d_{BR}^{-3}$, $\ell_M = d_{MR}^{-3}$, and $\ell_{i,k} = d_{i,k}^{-3}$, $\forall i, k (i \neq k)$, where $d_{BR}$ is the distance between the BS and RS, $d_{MR}$ is the distance between the RS and MSs, and $d_{i,k}$ is the distance between MS $i$ and MS $k$. All the small-scale fading coefficients are independently drawn from a circularly symmetric complex Gaussian distribution with zero mean and unit variance. The transmit power budgets of the BS, RS and the MSs are $P_B = 30$ dBm, $P_R = 20$ dBm, and $P_M = 0$ dBm, respectively. For the self-loop interference channel, we introduce a residual self-loop interference level factor $\xi$, which defines the ratio of the residual self-loop interference power to the noise power at each node, i.e., $\xi = \ell_{RL}\sigma_{RL}^2/\sigma^2 = \ell_{BL}\sigma_{BL}^2/\sigma^2 = \ell_{ML}\sigma_{ML}^2/\sigma^2$. Unless otherwise specified, we assume that there are $K = 8$ MSs; $d_{BR} = d_{MR} = 50$m, and $d_{i,k} = 30$m, $\forall i, k (i \neq k)$, respectively; the noise variance $\sigma^2 = -50$ dBm; and residual self-loop interference level factor $\xi = 0$ dB. We also plot the results of cut-set bound and a FD relaying scheme with maximum ratio combining and maximum ratio transmission (MRC/MRT) [31] for performance comparison.

Fig. 2 shows the achievable spectral efficiency of the proposed FD-DF and FD-AF under different numbers of antennas at the RS, i.e., $N_R$. The number of antennas at the BS is fixed to be $N_B = 200$. We also plot the spectral efficiency of HD-DF and HD-AF for comparison purpose. It is observed that the analytical results for FD-DF and FD-AF schemes asymptotically approach the simulation results. The FD-DF scheme is able to closely approaching the cut-set upper bound. For instance, the spectral efficiency gap is less than 3 bps/Hz when both the BS and the RS are equipped with 200 antennas. It can also be seen that despite the existence of residual self-loop interference, both FD-DF and FD-AF outperform their HD counterparts when the numbers of antennas are sufficient large, and their gains grow with $N_R$. For instance, FD-DF can achieve 70% higher spectral

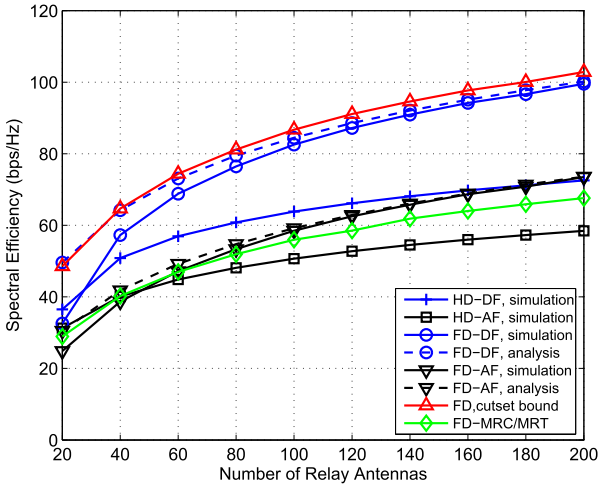


**FIGURE 2.** Spectral efficiency of FD-DF and FD-AF with $K = 8$ MSs. The BS is equipped with $N_B = 200$ antennas.

efficiency than HD-DF, when the RS is equipped with more than 100 antennas. Fig. 2 also confirms that FD-DF outperforms FD-AF. This is due to the fact that self-loop interference and noise at the RS propagate to the BS and MSs in FD-AF.

In Fig. 3, the spectral efficiency of FD-cTWRNs under different number of MSs is plotted, where $N_B = 200$ and $N_R = 100$. The other simulation parameters are the same as those in Fig. 2. As the number of MSs increases, each MS suffers from growing inter-user interference. Nevertheless, Fig. 3 demonstrates that the large antenna array is able to combat the growing ISI and improve the spectral efficiency of both FD-DF and FD-AF. It can also be seen that the performance gap between the proposed FD-DF scheme and the FD-MRC/MRT scheme enlarges as the number of users increases. This is due to the fact that MRC/MRT based linear processing suffers from ISI at all nodes, while the ISI is completely removed with zero-forcing receiving/precoding in FD-DF scheme.

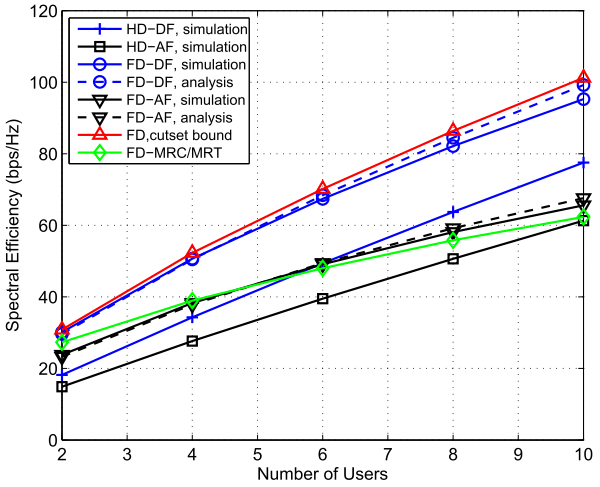


**FIGURE 3.** Spectral efficiency of FD-DF and FD-AF under different number of MSs. $N_B = 200$ and $N_R = 100$.

Fig. 4 investigates the impact of relay location on the spectral efficiency of the proposed two schemes. From the figure, we see that a higher spectral efficiency can be achieved for these schemes when the relay is close to the MSs. This is due to the fact that with large antenna arrays, the system throughput is bottlenecked by the RS-MS links in the FD-cTWRNs. It can be also seen that the gap between FD-DF and the cut-set bound is small in most cases.

Fig. 5 shows the impact of the residual self-loop interference on the spectral efficiency of FD-DF and FD-AF, where $K = 8$, and the other systems parameters are the same as those in Fig. 2. We see that in the case that the residual self-loop interference is weak, the spectral efficiencies of FD-DF and FD-AF can bypass those of HD-DF and HD-AF, respectively. In the case that the residual self-loop interference is strong, i.e., $\xi \geq 9$ dB, it is possible that FD-DF and FD-AF

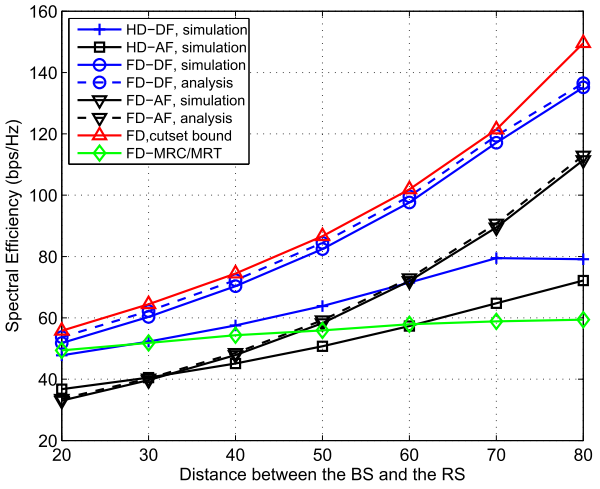


**FIGURE 4.** The impact of relay location on the spectral efficiency of FD-DF and FD-AF, $N_B = 200$ and $N_R = 100$.

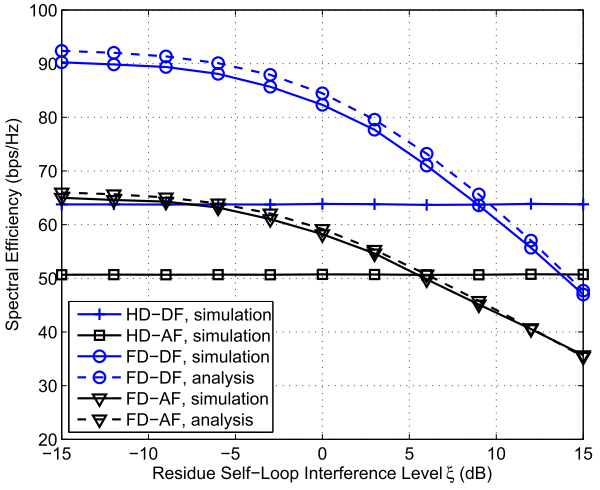


**FIGURE 5.** Spectral efficiency of FD-DF and FD-AF under different levels of residual self-loop interference, $N_B = 200$ and $N_R = 100$.

perform worse than their respective HD counterparts, for a given pair of $N_B$ and $N_R$. Nonetheless, it is noted that one can increase $N_R$ and/or $N_B$ to improve the robustness of FD-cTWRNs against self-loop interference. As long as the numbers of antennas at the BS and RS are sufficient large, the FD schemes is superior to their HD counterparts in terms of spectral efficiency.

Finally, Figs. 6 and 7 investigate the spectral efficiency of the two FD schemes in both the downlink and uplink, where power scaling is taken into account. Particularly, the transmit power of each MS is set to be inversely proportional to the number of antennas at the RS, i.e., $P_M = 1\ \text{mW}/N_R$, while the transmit powers of the BS and RS are fixed to be 30 dBm and 20 dBm, respectively. From the figures, we see that the achievable spectral efficiency in the downlink increases as the number of antennas increases at the RS. In contrast, the uplink spectral efficiency flats out and converges for both FD-DF and FD-AF. These results suggest that with FD and massive

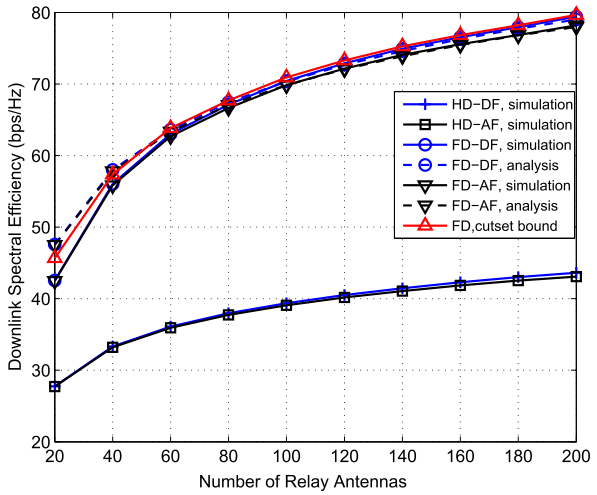


**FIGURE 6.** Downlink spectral efficiency of FD-DF and FD-AF under power scaling. The BS is equipped with $N_B = 200$ antennas.

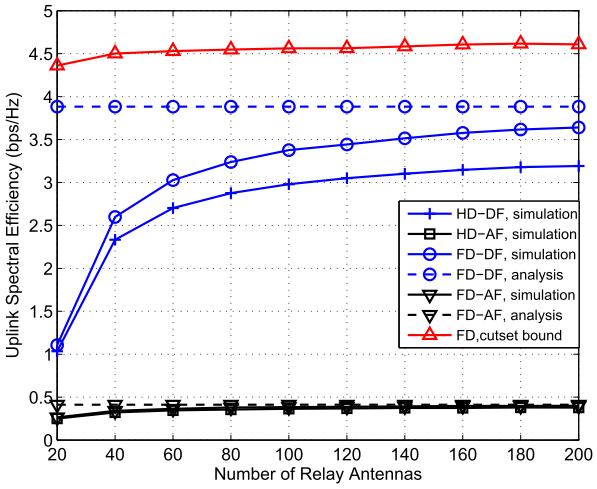


**FIGURE 7.** Uplink spectral efficiency of FD-DF and FD-AF under power scaling. The BS is equipped with $N_B = 200$ antennas.

MIMO, the transmit power of the MSs can be substantially reduced, while a prescribed data rate can be preserved, as revealed in Proposition 4.

## VI. CONCLUSIONS

In this paper, we analyzed the impact of FD and massive MIMO on the spectral efficiency of cTWRNs. Closed-from expressions were derived as the number of antennas become large. It was shown that massive MIMO is able to suppress self-loop interference and small-scaling fading, thereby improving the spectral efficiency of cTWRNs. We also proved that FD-cTWRNs can always outperform their HD counterparts in the presence of massive MIMO at the BS and RS. In our future work, we will extend these results to the case where channel state information is imperfect at both the BS and RS. The proposed FD-DF and FD-AF relaying protocols can also be applied to energy-harvesting networks [33]–[35].

## APPENDIX A
## PROOF OF PROPOSITION 1

First, given the receive SINR $\gamma_{BR,k}$, the variance of the noise $\boldsymbol{w}_{RR,k}^H \boldsymbol{z}_R$ in (11) can be given by

$$\begin{aligned}\mathbb{V}\mathrm{ar}\left[\boldsymbol{w}_{RR,k}^H \boldsymbol{z}_R\right] &= \sigma^2 \mathbb{E}[\|\boldsymbol{w}_{RR,k}\|^2] \\ &= \sigma^2 \mathbb{E}\left[\left((\boldsymbol{H}_{SR}^H \boldsymbol{H}_{SR})^{-1}\right)_{kk}\right] \\ &= \frac{\sigma^2}{K\ell_B} \mathbb{E}\left[\mathrm{tr}\left((\tilde{\boldsymbol{H}}_{SR}^H \tilde{\boldsymbol{H}}_{SR})^{-1}\right)\right] \\ &= \frac{\sigma^2}{(N_R - K)\ell_B}, \end{aligned} \tag{46}$$

where $k = 1, \ldots, K$, and the identity $\mathbb{E}\left[\mathrm{tr}(\boldsymbol{X}^{-1})\right] = \frac{M}{N-M}$ in the case that $\boldsymbol{X}$ is a $M \times M$ central Wishart matrix with $N$ degrees-of-freedom [32], are used in the last equality. Substituting (13) and (46) into (11), we achieve (24a).

Likewise, the variance of the noise in (12) can be given by

$$\mathbb{V}\mathrm{ar}\left[\boldsymbol{w}_{RR,K+k}^H \boldsymbol{z}_R(n)\right] = \frac{\sigma^2}{(N_R - K)\ell_M}, \quad k = 1, \ldots, K. \tag{47}$$

Substituting (14) and (47) into (12), we obtain (24b).

Next, consider the receive SINRs at the BS. With large antenna arrays at the BS and RS, from (16), $\alpha_R^{\mathrm{DF}}$ can be determined by [24]

$$\begin{aligned}\alpha_R^{\mathrm{DF}} &= \sqrt{\frac{P_R}{K\ell_M \mathbb{E}\left\{\mathrm{tr}\left[\left(\boldsymbol{H}_{RM}\boldsymbol{H}_{RM}^H\right)^{-1}\right]\right\}}} \\ &= \sqrt{\frac{(N_R - K)\ell_M P_R}{K}}. \end{aligned} \tag{48}$$

For the receive SINRs at the BS, the variance of the noise $\boldsymbol{w}_{B,k}^H \boldsymbol{z}_B(n)$ in (19) can be given by

$$\begin{aligned}&\mathbb{V}\mathrm{ar}\left[\boldsymbol{w}_{B,k}^H \boldsymbol{z}_B(n)\right] \\ &= \sigma^2 \mathbb{E}\left[\|\boldsymbol{w}_{B,k}\|^2\right] \\ &= \sigma^2 \mathbb{E}\left\{\left[\left(\left(\boldsymbol{H}_{RB}\boldsymbol{H}_{RM}^\dagger\right)^H \left(\boldsymbol{H}_{RB}\boldsymbol{H}_{RM}^\dagger\right)\right)^{-1}\right]_{k,k}\right\} \\ &= \frac{\ell_M N_R \sigma^2}{\ell_B N_B}. \end{aligned} \tag{49}$$

Substituting (48), (49) and (20) into (19), we achieve (24c).

For the receive SINRs at the MSs, in the case that there are a large number of MSs, we have

$$|h_{k,k}|^2 \sigma_{ML}^2 + P_M \sum_{i \neq k} |h_{i,k}|^2 \simeq P_M \sum_{i=1}^{K} \ell_{i,k}. \tag{50}$$

Finally, we can obtain (24d) by substituting (48) and (50) into (22).

## APPENDIX B
## PROOF OF PROPOSITION 2

With large antenna arrays at the BS and RS, from (25), $\alpha_B$ can be determined by

$$\alpha_B = \sqrt{\frac{P_B}{\mathbb{E}\left\{\mathrm{tr}\left[\left(\boldsymbol{H}_{MR}^{\dagger}\boldsymbol{H}_{BR}\right)^{\dagger}\left(\left(\boldsymbol{H}_{MR}^{\dagger}\boldsymbol{H}_{BR}\right)^{\dagger}\right)^{H}\right]\right\}}} = \sqrt{\frac{\ell_B N_B P_B}{\ell_M K N_R}}. \tag{51}$$

From (3) and (26), $\alpha_R^{\mathrm{AF}}$ can be given by

$$\alpha_R^{\mathrm{AF}} = \sqrt{\frac{P_R}{(\alpha_B^2 + P_M + \Delta_1 + \Delta_2)\mathbb{E}\left\{\mathrm{tr}\left[\boldsymbol{H}_{RM}^{\dagger}\boldsymbol{H}_{RM}^{\dagger H}\right]\right\}}}. \tag{52}$$

where

$$\Delta_1 = \sigma^2\mathbb{E}\left\{\mathrm{tr}\left[\boldsymbol{H}_{MR}^{\dagger}\boldsymbol{H}_{MR}^{\dagger H}\right]\right\}, \tag{53}$$

and

$$\Delta_2 = \sigma_{RL}^2\mathbb{E}\left\{\mathrm{tr}\left[\boldsymbol{H}_{MR}^{\dagger}\boldsymbol{H}_{RR}\boldsymbol{H}_{RR}^{H}\boldsymbol{H}_{MR}^{\dagger H}\right]\right\} \tag{54}$$

are the powers of the noise and self-loop interference after ZFBF, respectively.

Given a large number of antennas at the RS, we have

$$\Delta_1 = \sigma^2\mathbb{E}\left\{\mathrm{tr}\left(\boldsymbol{H}_{MR}^{\dagger}\boldsymbol{H}_{MR}^{\dagger H}\right)\right\} = \frac{K}{N_R - K}\ell_M^{-1}\sigma^2, \tag{55}$$

which becomes negligible ($\Delta_1 \to 0$ if $N_R \to +\infty$).

Similarly, we have

$$\Delta_2 = \sigma_{RL}^2\ell_{RL}P_R\mathbb{E}\left\{\mathrm{tr}\left(\boldsymbol{H}_{MR}^{\dagger}\boldsymbol{H}_{MR}^{\dagger H}\right)\right\} = \frac{K}{N_R - K}\ell_M^{-1}\ell_{RL}P_R, \tag{56}$$

which can also be negligible when $N_R \to +\infty$.

Then, $\alpha_R^{\mathrm{AF}}$ in (52) can be approximated by

$$\alpha_R^{\mathrm{AF}} \simeq \sqrt{\frac{P_R}{(\alpha_B^2 + P_M)\mathbb{E}\left\{\mathrm{tr}\left[\boldsymbol{H}_{RM}^{\dagger}\boldsymbol{H}_{RM}^{\dagger H}\right]\right\}}} = \sqrt{\frac{(N_R - K)\ell_M P_R}{K(\alpha_B^2 + P_M)}}. \tag{57}$$

For the receive SINR at MS $k$, the variance of the noise in (30) can be given by

$$\rho_{R,k} = \sigma^2\mathbb{E}\left[\left((\boldsymbol{H}_{MR}^{H}\boldsymbol{H}_{MR})^{-1}\right)_{kk}\right] = \frac{\sigma^2}{(N_R - K)\ell_M}. \tag{58}$$

The variance of the self-loop interference at MS $k$ can be given by

$$\mu_{R,k} = \ell_{RL}P_R\mathbb{E}\left[\left((\boldsymbol{H}_{MR}^{H}\boldsymbol{H}_{MR})^{-1}\right)_{kk}\right] = \frac{\ell_{RL}P_R}{(N_R - K)\ell_M}. \tag{59}$$

Substituting (51) and (57)-(59) into (30), we obtain (32b).

For the receive SINRs at the BS, the variance of the noise $\boldsymbol{w}_{B,k}^{H}\boldsymbol{H}_{BB}\tilde{\boldsymbol{x}}_B(n)$ in (29) can be given by

$$\tilde{\sigma}_{B,k}^2 = \sigma_{BL}^2\mathbb{E}\left[\boldsymbol{w}_{B,k}^{H}\boldsymbol{H}_{BB}\boldsymbol{H}_{BB}^{H}\boldsymbol{w}_{B,k}\right] = \sigma_{BL}^2 N_B\ell_{BL}\mathbb{E}\left[\|\boldsymbol{w}_{B,k}\|^2\right] = \frac{\ell_M N_R\ell_{BL}P_B}{\ell_B N_B}. \tag{60}$$

Substituting(49), (51), (57) and (60) into (29), we can finally obtain (32a).

## REFERENCES


[1] J. Choi, M. Jain, K. Srinivasan, P. Levis, and S. Katti, "Achieving single channel, full duplex wireless communication," in *Proc. Mobicom*, New York, NY, USA, Sep. 2010, pp. 1–12.

[2] D. Bharadia, E. McMilin, and S. Katti, "Full duplex radios," in *Proc. ACM SIGCOMM*, Hong Kong, Aug. 2013, pp. 375–386.

[3] D. Kim, H. Lee, and D. Hong, "A survey of in-band full-duplex transmission: From the perspective of PHY and MAC layers," *IEEE Commun. Surveys Tuts.*, vol. 17, no. 4, pp. 2017–2046, 4th Quart., 2015.

[4] G. Liu, F. R. Yu, H. Ji, V. C. M. Leung, and X. Li, "In-band full-duplex relaying: A survey, research issues and challenges," *IEEE Commun. Surveys Tuts.*, vol. 17, no. 2, pp. 500–524, 2nd Quart., 2015.

[5] Z. Zhang, K. Long, A. V. Vasilakos, and L. Hanzo, "Full-duplex wireless communications: Challenges, solutions, and future research directions," *Proc. IEEE*, vol. 104, no. 7, pp. 1369–1409, Jul. 2016.

[6] T.-X. Zheng, H.-M. Wang, Q. Yang, and M. H. Lee, "Safeguarding decentralized wireless networks using full-duplex jamming receivers," *IEEE Trans. Wireless Commun.*, vol. 16, no. 1, pp. 278–292, Jan. 2017.

[7] Q. Cui, Y. Zhang, W. Ni, M. Valkama, and R. Jantti, "Energy efficiency maximization of full-duplex two-way relay with non-ideal power amplifiers and non-negligible circuit power," *IEEE Trans. Wireless Commun.*, vol. 16, no. 9, pp. 6264–6278, Sep. 2017.

[8] Q. Cui, T. Yuan, and W. Ni, "Energy-efficient two-way relaying under non-ideal power amplifiers," *IEEE Trans. Veh. Technol.*, vol. 66, no. 2, pp. 1257–1270, Feb. 2017.

[9] T. L. Marzetta, "Noncooperative cellular wireless with unlimited numbers of base station antennas," *IEEE Trans. Wireless Commun.*, vol. 9, no. 11, pp. 3590–3600, Nov. 2010.

[10] H. Q. Ngo, E. G. Larsson, and T. L. Marzetta, "Energy and spectral efficiency of very large multiuser MIMO systems," *IEEE Trans. Commun.*, vol. 61, no. 4, pp. 1436–1449, Apr. 2013.

[11] T. Riihonen, S. Werner, and R. Wichman, "Mitigation of loopback self-interference in full-duplex MIMO relays," *IEEE Trans. Signal Process.*, vol. 59, no. 12, pp. 5983–5993, Dec. 2011.

[12] E. Ahmed and A. M. Eltawil, "All-digital self-interference cancellation technique for full-duplex systems," *IEEE Trans. Wireless Commun.*, vol. 14, no. 7, pp. 3519–3532, Jul. 2014.

[13] M. Heino *et al.*, "Recent advances in antenna design and interference cancellation algorithms for in-band full duplex relays," *IEEE Commun. Mag.*, vol. 53, no. 5, pp. 91–101, May 2015.

[14] X. Zhang, W. Cheng, and H. Zhang, "Full-duplex transmission in PHY and MAC layers for 5G mobile wireless networks," *IEEE Wireless Commun.*, vol. 22, no. 5, pp. 112–121, May 2015.

[15] E. Hossain and M. Hasan, "5G cellular: Key enabling technologies and research challenges," *IEEE Instrum. Meas. Mag.*, vol. 18, no. 3, pp. 11–21, Jun. 2015.

[16] F. Rusek *et al.*, "Scaling up MIMO: Opportunities and challenges with very large arrays," *IEEE Signal Process. Mag.*, vol. 30, no. 1, pp. 40–46, Jan. 2013.

[17] E. G. Larsson, O. Edfors, F. Tufvesson, and T. L. Marzetta, "Massive MIMO for next generation wireless systems," *IEEE Commun. Mag.*, vol. 52, no. 2, pp. 186–195, Feb. 2014.
[18] B. Rankov and A. Wittneben, "Spectral efficient protocols for half-duplex fading relay channels," *IEEE J. Sel. Areas Commun.*, vol. 25, no. 2, pp. 379–389, Feb. 2007.
[19] H. J. Yang, J. Chun, and A. Paulraj, "Asymptotic capacity of the separated MIMO two-way relay channel," *IEEE Trans. Inf. Theory*, vol. 57, no. 11, pp. 7542–7554, Nov. 2011.
[20] X. Yuan, T. Yang, and I. B. Collings, "Multiple-input multiple-output two-way relaying: A space-division approach," *IEEE Trans. Inf. Theory*, vol. 59, no. 10, pp. 6421–6440, Oct. 2013.
[21] H. J. Yang, Y. Choi, N. Lee, and A. Paulraj, "Achievable sum-rate of MU-MIMO cellular two-way relay channels: Lattice code-aided linear precoding," *IEEE J. Sel. Areas Commun.*, vol. 3, no. 8, pp. 1304–1318, Sep. 2012.
[22] Z. Fang, X. Yuan, and X. Wang, "Towards the asymptotic sum capacity of the MIMO cellular two-way relay channel," *IEEE Trans. Signal Process.*, vol. 62, no. 16, pp. 4039–4051, Aug. 2014.
[23] Z. Fang, F. Liang, J. Li, L. Jin, and Y. Liu, "Multiuser two-way relaying with large-scale antenna arrays and energy harvesting," *Wireless Pers. Commun.*, vol. 95, no. 2, pp. 1299–1315, Jul. 2017.
[24] Z. Fang, X. Yuan, X. Wang, and C. Li, "Nonregenerative cellular two-way relaying with large-scale antenna arrays," *IEEE Trans. Veh. Technol.*, vol. 65, no. 7, pp. 4959–4972, Jul. 2016.
[25] L. Jimenez Rodriguez, N. H. Tran, and T. Le-Ngoc, "Optimal power allocation and capacity of full-duplex AF relaying under residual self-interference," *IEEE Wireless Commun. Lett.*, vol. 3, no. 2, pp. 233–236, Apr. 2014.
[26] H. Q. Ngo, H. A. Suraweera, M. Matthaiou, and E. G. Larsson, "Multipair full-duplex relaying with massive arrays and linear processing," *IEEE J. Sel. Areas Commun.*, vol. 32, no. 9, pp. 1721–1737, Sep. 2014.
[27] H. Cui, M. Ma, L. Song, and B. Jiao, "Relay selection for two-way full duplex relay networks with amplify-and-forward protocol," *IEEE Trans. Wireless Commun.*, vol. 13, no. 7, pp. 3768–3777, Jul. 2014.
[28] Q. Li and D. Han, "Sum secrecy rate maximization for full-duplex two-way relay networks," in *Proc. ICASSP*, Mar. 2016, pp. 3641–3645.
[29] X. Xia, W. Xie, D. Zhang, K. Xu, and Y. Xu, "Multi-pair full-duplex amplify-and-forward relaying with very large antenna arrays," in *Proc. WCNC*, Mar. 2015, pp. 304–309.
[30] X. Jia, P. Deng, L. Yang, and H. Zhu, "Spectrum and energy efficiencies for multiuser pairs massive MIMO systems with full-duplex amplify-and-forward relay," *IEEE Access*, vol. 3, pp. 1907–1918, 2015.
[31] Z. Zhang, Z. Chen, M. Shen, and B. Xia, "Spectral and energy efficiency of multipair two-way full-duplex relay systems with massive MIMO," *IEEE J. Sel. Areas Commun.*, vol. 34, no. 4, pp. 848–863, Apr. 2016.
[32] A. M. Tulino and S. Verdú, "Random matrix theory and wireless communications," *Found. Trends Commun. Inf. Theory*, vol. 1, no. 1, pp. 1–182, 2004.
[33] X. Chen, W. Ni, X. Wang, and Y. Sun, "Provisioning quality-of-service to energy harvesting wireless communications," *IEEE Commun. Mag.*, vol. 53, no. 4, pp. 102–109, Apr. 2015.
[34] Z. Nan, T. Chen, X. Wang, and W. Ni, "Energy-efficient transmission schedule for delay-limited bursty data arrivals under nonideal circuit power consumption," *IEEE Trans. Veh. Technol.*, vol. 65, no. 8, pp. 6588–6600, Aug. 2016.
[35] X. Chen, W. Ni, X. Wang, and Y. Sun, "Optimal quality-of-service scheduling for energy-harvesting powered wireless communications," *IEEE Trans. Wireless Commun.*, vol. 15, no. 5, pp. 3269–3280, May 2016.

**ZHAOXI FANG** (M'15) received the B. Eng. in communication engineering and the Ph.D. degree in electrical engineering from Fudan University, Shanghai, China, in 2004 and 2009, respectively. In 2009, he joined the School of Electronics and Computer, Zhejiang Wanli University, Ningbo, China, where he is currently a Professor. From 2013 to 2014, he was a Post-Doctoral Researcher with the Department of Electrical and Computer Engineering, Michigan State University, USA. His research interests include multiple-input multiple-output, communications, wireless relaying, and cooperative communications.

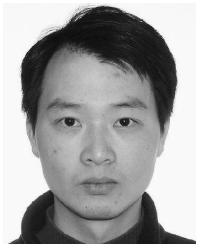

**WEI NI** (M'09–SM'15) received the B.E. and Ph.D. degrees in electronic engineering from Fudan University, Shanghai, China, in 2000 and 2005, respectively. He was a Deputy Project Manager with the Bell Labs R&I Center, Alcatel/Alcatel-Lucent from 2005 to 2008, and a Senior Researcher with Devices Research and Development, Nokia from 2008 to 2009. He is currently a Team Leader, a Project Leader, and a Senior Scientist with CSIRO, Australia. He also holds adjunct position at Macquarie University, Sydney, and the University of Technology Sydney, Sydney. His research interests include radio resource management, software-defined networking, network security, and multiuser MIMO. He also served as the Publication Chair of BodyNet 2015, Student Travel Grant Chair for WPMC 2014, Program Committee Member of CHINACOM 2014, and TPC member of the IEEE ICC'14, the ICCC'15, the EICE'14, and the WCNC'10. He serves as an Editorial Board Member for *Hindawi Journal of Engineering* (2012–2014), *Secretary of IEEE NSW VTS Chapter* (2015–2016), Track Chair of the IEEE VTC-Spring 2017, and PHY Track Co-chair of the IEEE VTC-Spring 2016.

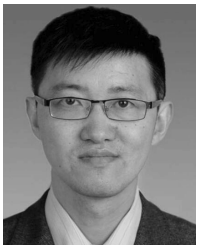

**FENG LIANG** received the B.S. and M.S. degrees in optical instruments from Zhejiang University, China, in 1989 and 1992, respectively, and Ph.D. degree in optical instruments from the Shanghai Institute of Optics and Fine Mechanics, Chinese Academy of Sciences, in 1995. He is currently the Dean with the School of Electronics and Computer, Zhejiang Wanli University, China. He has authored and co-authored over 30 technical papers in journals. His current interests focus on network security, QoS of WLAN, network management systems, and multimedia communications.

**PENGFEI SHAO** received the B.E. and M.S. degrees in communication and information system from the Beijing University of Posts and Telecommunications in 2000 and 2003, respectively, and the Ph.D. degree in control theory and control engineering from the Zhejiang University of Technology in 2016. He is currently an Associate Professor with the School of Electronics and Computer, Zhejiang Wanli University, Ningbo, China. His research interests include wireless networking and information fusion.

**YAOHUI WU** received the B.E. and M.S. degrees in communication engineering from the Beijing University of Posts and Telecommunications, China in 2001 and 2004, respectively. He is currently pursuing the Ph.D. degree in communication engineering with Ningbo University. He is also with the School of Electronics and Computer, Zhejiang Wanli University. His research interests include resource allocation and channel estimation.